Research article

Journal of RAMAN SPECTROSCOPY

Received: 14 March 2014 Revised: 27 June 2014 Accepted: 3 July 2014 Published online in Wiley Online Library: 7 August 2014

(wileyonlinelibrary.com) DOI 10.1002/jrs.4558

Intricate packing in the hydrophobic core of barstar through a CH–π interaction

Erix A. Milán-Garcés,[a] Sayan Mondal,[b] Jayant B. Udgaonkar[a] and Mrinalini Puranik[b]*

Identification of specific packing interactions within in the hydrophobic core of proteins is important for understanding the integrity of protein structure. Finding such interactions is challenging because few tools allow monitoring of a specific interaction in the presence of several non-specific forces that hold proteins together. It is important to understand how and when such interactions develop during protein folding. In this study, we have used the intrinsic tryptophan residue, Trp53, as an ultraviolet resonance Raman probe to elucidate the packing interactions in the hydrophobic core of the protein barstar. Barstar is extensively studied for its folding, unfolding and aggregation properties. The Trp53 residue is known to be completely buried in the hydrophobic core of the protein and is used extensively as an intrinsic probe to monitor the folding and unfolding reactions of barstar. A comparison of the resonance Raman cross sections of some bands of Trp53 with those observed for N-acetyl-tryptophanoamide in water suggests that Trp53 in barstar is indeed isolated from water. Intensity ratio of the Fermi doublet suggests that Trp53 is surrounded by several aliphatic amino acid residues in corroboration with the crystal structure of barstar. Importantly, we show that the side chain of Trp53 is involved in a unique CH–π interaction with CH groups of Phe56 as well as a steric interaction with the methyl group of Ile5. Copyright © 2014 John Wiley & Sons, Ltd.

Additional supporting information may be found in the online version of this article at the publisher's web site.

Keywords: UV resonance Raman spectroscopy; tryptophan; CH–π interactions; packing interactions

Introduction

The stability and native structure of a protein are maintained by a complex network of interactions including hydrophobic interactions, hydrogen bonding, electrostatic and packing interactions. Although the hydrophobic effect is considered to contribute most to the stability and folding of proteins,[1] packing interactions also play an important role.[2–5] In an early survey of protein structures, it was found that proteins are packed with densities similar to those of crystals of small organic molecules.[6–8] The higher packing density in proteins in comparison to liquids suggests that van der Waals forces make an important contribution to the stability of proteins. Mutations that resulted in the creation of large cavities inside the core were found to destabilize the native state due to a decrease in strength of the van der Waals interactions.[9–13] The role of these weak interactions is also important in protein folding and in stabilizing intermediates on the folding pathway, e.g. in the structures of dry molten globule intermediates found in a few proteins.[14–18] In the dry molten globule, a structurally expanded form of the native protein, the packing density is loose as compared to the native state but van der Waals interactions are still strong enough to prevent penetration of water into the core. These studies suggest that the core packing interactions are the first to be lost during unfolding and are the last to form during folding reaction of the proteins.[14,19]

Barstar is an inhibitor of the ribonuclease barnase, and its structure and folding have been systematically explored.[19–29] Packing interactions in the barstar core have been characterized using different experimental and theoretical studies.[22,25,29–32] Calorimetric measurements of the enthalpy and entropy changes of barstar denaturation suggested that the native state conformation is more loosely packed than the native state conformations of other proteins.[32] Molecular dynamics (MD) simulations too report a highly dynamic core.[30] Nuclear magnetic resonance (NMR) spectroscopy studies have shown that the side chain of Phe74 in the hydrophobic core of barstar is able to flip without constraint.[29,30,33] In contrast, Phe56 is in a rigid environment, possibly due to its interaction with Trp53.[29]

Wt barstar contains three tryptophan (Trp) residues, with one Trp (Trp53) completely buried in the core. A mutant form of barstar that contains only Trp53 has been extensively used for fluorescence spectroscopy-based studies. The fluorescence of Trp53 decays with single exponential characteristics with a lifetime of 4.9 ns against the typical biexponential decay observed for free Trp in water.[25] Time-resolved fluorescence anisotropy decay measurements of Trp53 in this mutant protein showed a single rotational correlation time of 4.1 ns that corresponds to the global tumbling of the protein. Thus, Trp53 is in a rigid local environment that constrains the rotation of the side chain so that within the protein it exists in a single rotational isomer. The rigidity of Trp53 was also confirmed by a NMR study carried out by Li *et al.*[29]

* *Correspondence to: Mrinalini Puranik, Indian Institute of Science Education and Research, Mendeleev, Dr. Homi Bhabha Road, Pune 411 008, India. E-mail: mrinalini@iiserpune.ac.in; puranik.mrinalini@gmail.com*

a *National Centre for Biological Sciences, Tata Institute of Fundamental Research, Bangalore 560065, India*

b *Indian Institute of Science Education and Research, Pune, 411008, India*

The differences in the dynamics of Phe74, Phe56 and Trp53 indicate that the packing density in the core of barstar is not homogeneous. Packing interactions are stronger in the region of the core around Trp53 and Phe56 than in other regions. This also suggests that the van der Waals interactions between these two amino acid residues are strong in the native state. Further evidence for the importance of the interaction between these residues was provided by the cold denaturation studies of barstar by Wong *et al.*[34] They found that three regions form non-random residual structures in the denatured state of barstar, and that Trp53 and Phe56 are part of one of these regions. Despite these extensive studies and its central role in the structure of barstar, the precise nature of the interaction between Trp53 and Phe56 is not understood.

Barstar is extensively used as a model to examine the sequence of structural events during folding—hydrophobic collapse, packing, formation of secondary and tertiary structures. Kinetics studies indicate that the initial event during the folding of barstar is a hydrophobic collapse to a globule form with a solvated core and no appreciable secondary structure.[20] Sridevi *et al.* studied the slow stage of the folding reaction of barstar and determined the sequence of events during the formation of significant secondary and tertiary structure. The formation of native-like packing interactions in the hydrophobic core preceded these events.[22] During the salt-induced refolding reaction of barstar at pH12, the protein transforms to a molten globule with a consolidated core while the secondary and tertiary structure attains 65 and 40%, respectively, of that of the native state.[22–24] Thus, it appears that assembly of the hydrophobic core is central to understanding the folding of barstar.

To characterize the packing interactions that confer rigidity to Trp53 in the core, we have employed ultraviolet resonance Raman spectroscopy (UVRR). UVRR allows selective observation of Trp residues through resonance enhancement. Raman excitation within the electronic absorption band of Trp at around 230 nm enhances the Trp Raman bands, without enhancing contributions from amide vibrations.[35–38] This provides a powerful, intrinsic, label-free method to monitor changes in the local environment of these amino acid residues.[39–53] The ability to selectively observe Trp residues is valuable in studying the structure of the protein core, as Trp is frequently found in protein interiors and has a large surface area.

Here, we report the first UVRR spectra of wild type barstar as well as of a single Trp-containing mutant form of barstar. Unique spectral signatures of Trp53 were identified by comparing the spectra of the wt protein and a single Trp-containing mutant form. The spectra reconfirm the previous conclusion that Trp53 is in a hydrophobic environment that is devoid of solvent. We find that a unique CH–π interaction of Trp53 with Phe56 constrains rotation of the rings of both amino acid residues. The experimental results have been supported by quantum chemical calculations using density functional theory (DFT). This is the first experimental detection of CH–π interactions between the aromatic rings of Trp and Phe inside proteins using Raman spectroscopy. CH–π interactions have been found to be crucial in the stabilities and functions of proteins.[54–63] Quantum chemical calculations have established that CH–π interactions are similar in nature to van der Waals interactions with the major contribution arising from dispersion forces.[54,64–66] An important additional feature of CH–π interactions is their directionality because of which they are likely to play a more specific role in the protein architecture than other non-specific van der Waals interactions. The current results will facilitate future time-resolved and pH-dependent studies for monitoring the formation of initial contacts in the core during the folding of barstar.

Materials and methods

Preparation of samples

We have followed a procedure for the over-expression and purification of barstar that has been described previously.[67] The barstar variant (W38FW44FC82A) with a single Trp and a single Cys at the positions 53 and 40, respectively, was made by site-directed mutagenesis.[26,68]The purification procedure for this variant was as described earlier.[26,68] The single Trp containing mutant of Barstar, W38FW44FC82A, was made on the existing C82A background to avoid fluorescence/Raman interference from the surface Trp residues during monitoring of the core Trp residue. Since many of the studies on folding and unfolding of barstar protein using other structural probes (fluorescence resonance energy transfer and pulse-labeling methods) have used this mutant[19,69–73] it is used for the current study as well. It is also noted that Cys82 appears to interact with Lys78, Tyr47, and Ala77 residues.[19] Post-purification, barstar was stored as a dry lyophilized powder and dissolved in sodium phosphate buffer (0.1 M sodium phosphate buffer 1.0 mM EDTA, 0.1 M DTT and 0.2 M sodium perchlorate) at pH 7. Sodium perchlorate was added for use as an internal intensity standard in the Raman spectra. Typically, protein samples were at a concentration of 200-μM barstar. N-acetyl-tryptophanoamide (NATA) was purchased from Sigma Aldrich and used as received. For Raman experiments, NATA (1.0 mM) was dissolved in the same buffer as described above for barstar. For deuterium labeling, the protein was dissolved in phosphate buffer prepared in D_2O at pD7and incubated overnight.

UVRR

Resonance Raman spectra were recorded with the 229-nm excitation wavelength produced as the output of the fourth harmonic of a Ti:sappahire laser (Ti–S). The Ti–S was in turn pumped by a Nd:YLF laser (Photonics Industries, Bohemia, NY). Samples were placed in NMR tubes that were spun about their axes to minimize photodamage. The typical laser power at the sample was 0.6 mW. The scattered light was focused into a monochromator SPEX 1250 M, JobinYvon (3600 grooves/mm) and detected on a 1024×256 pixels CCD camera, JobinYvon. The spectrum of each sample corresponds to the average of three sets of fresh samples with a total of 6-min exposure of the CCD for each sample. The integrity of the samples in laser light was confirmed by comparing the spectra at the first and last scan for a given sample. No appreciable difference in the spectra was found. Spectra were calibrated using the known band positions of standard solvents: cyclohexane, acetonitrile and isopropyl alcohol. Positions and intensities were determined by fitting Lorentzian functions to the bands in the spectra. The total differential Raman cross sections $(\partial\sigma_N/\partial\Omega)_{\parallel+\perp}$ of the bands of NATA and Trp53 were determined from the formula[69]:

$$\left(\frac{\partial\sigma_N}{\partial\Omega}\right)_{II+\perp} = \left(\frac{I_N}{I_S}\right)\left(\frac{C_S}{C_N}\right)\left(\frac{\partial\sigma_S}{\partial\Omega}\right)_{II+\perp}$$

where S and N correspond to the bands of the internal standard and of the sample. C and I stand for the concentration and

intensity (area), respectively, and $(\partial\sigma_S/\partial\Omega)_{II+\perp}$ represents the known value of total differential cross section of the internal standard (sodium perchlorate).[70]

Computational methods

Environment and interactions of Trp 53 in the core of barstar were modeled using a pure quantum mechanical model that included the complete, neutral amino acids: Trp53, Phe56 and Ile5. The calculations were performed with Gaussian09 program[74] package using DFT. To study the non-covalent interactions, the dispersion corrected density functional wb97xD[71] was used. wB97xD functional is a long range hybrid functional with empirical dispersion correction (going down in a $1/r^6$ pattern) and is one of the vastly used DFT choices for non-covalent complexes.[72,73] We used a moderately sized Pople triple split valence basis set 6311 + G (d,p) with polarization and diffuse functions on heavy atoms and polarization functions on hydrogen atoms for building potential energy surfaces (PES).

Three important coordinates have been chosen to observe for a close understanding of non-covalent interaction in the complex. These coordinates are (1) CH–π distance ($R_{CH-\pi}$) between CH group of Phe56 and center of mass of the benzene of Trp53 (Fig. S1 (Supporting Information)), (2) orientation of the Phe56 ring with respect to plane of π cloud of Trp53, i.e. dihedral angle ($\phi_{Phe-Trp}$) between atom H42, C32, C33 and C34 (Fig. S2 (Supporting Information)) and (3) CH–pyrrole distance (R_{CH-Py}) between CH of methyl group of Ile5 and center of mass of pyrrole ring of Trp53 (Fig. S3 (Supporting Information)).

Rigid PES scans along these three coordinates were constructed by calculating single point energy at different coordinate values. During this 1-D rigid PES scan, all the atoms were kept fixed, and only the required coordinate was changed in steps to generate the potential wells. For CH–π and CH–Py distances the step size was 0.1 Å and for Phe rotation, the step size was of 2°. After locating the minimum along these coordinates, a constrained geometry optimization without symmetry constraint was carried out. For this step, we used a relatively smaller Pople double split valence basis set 6-31G(d,p) with polarization functions on hydrogen and heavier atoms. Vibrational wavenumbers were computed at the same level to ensure that the associated structures are true minima. No imaginary wavenumbers were found.

As a first step, coordinates of Trp53 and Phe56 were extracted from PDB file 1A19, and the charge of the backbone was neutralized. The minimum energy structure of the Trp53–Phe56 complex was obtained. During the minimization, all internal coordinates of Phe56 and those of the backbone of Trp53 were constrained to crystal structure values. (See detailed description in Fig. 1 and Fig. 2 of Supplementary Material). With this structure as the initial input, a rigid PES scan along CH–π and $\phi_{Phe-Trp}$ coordinate was carried out as described above, and the structure of the complex with minimum energy was found.

In the next step, Ile5 was introduced into the energy minimized Trp53–Phe56 complex to form the final complete model consisting of Trp53–Phe56–Ile5. A further constrained geometry optimization of this complex was done in which Phe56 and Ile5 residues were kept fixed along with the backbone of Trp53, while the positions of the atoms of the indole ring of Trp53 were allowed to change. The minimum energy structure of this complex was obtained. A rigid PES scan was now performed by varying the CH–py distance between Ile5 and Trp53. During this latter scan, the Trp53–Phe56 distance was not varied and kept fixed at the minima of the Trp53–Phe56 complex ($R_{CH-\pi}$ = 2.74 Å and $\phi_{Phe-Trp}$ = 160.5°).

Results and discussion

UVRR spectra of wt barstar, the barstar variant -W38FW44FC82A and the Trp analogue, NATA are obtained with Raman excitation at a wavelength of 229 nm and are shown in Fig. 1. The main contributions to the spectra arise from Trp and Tyr residues, with negligible contribution from other residues of the protein or the amide backbone. Wt barstar has three Trp residues (Trp38, Trp44 and Trp53) and three Tyr residues (Tyr29, Tyr30 and Tyr47). In the mutant protein, Trp38 and Trp44 are replaced by Phe, while Cys82 has been substituted with Ala. Table 1 includes the positions of the Raman bands of Trp residues of the wt and mutant of barstar as well as for NATA in water.

Comparison of the spectrum of wt barstar to that of NATA shows that bands corresponding to Trp residues are altered in barstar. Major changes occur in the W18 region where two new bands appear: one at 780 cm^{-1} and the other in the form of a shoulder at 746 cm^{-1}. In addition to the changes in band position, there is also a decrease in the relative intensity of the W18 mode with respect to that of the W16 and W3 modes in the protein. The W10 mode downshifts from 1233 cm^{-1} in NATA

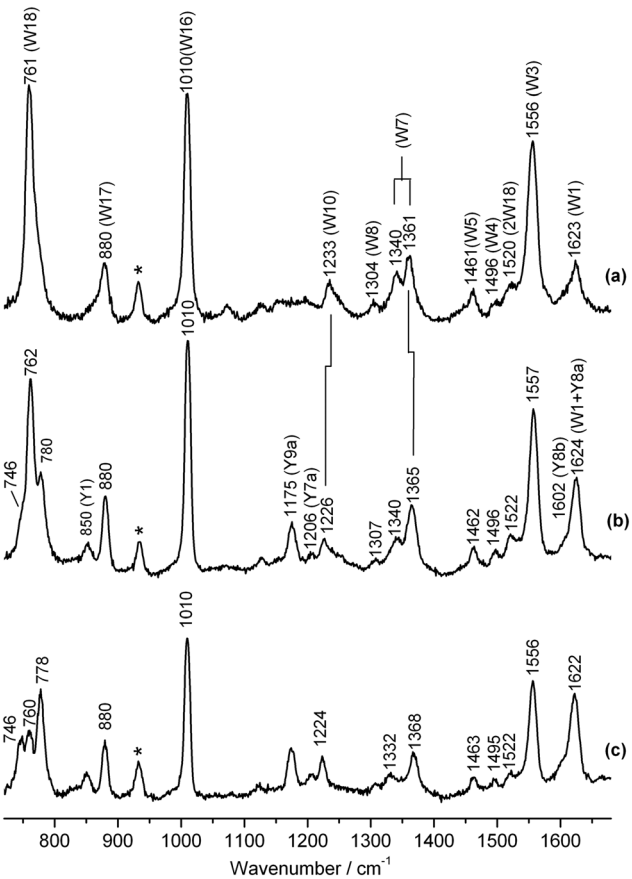

Figure 1. UVRR spectra of: (a) NATA (1.0 mM); (b) wt barstar (2.0 mg/ml) and (c) W38FW44FC82A mutant variant of barstar (2.0 mg/ml), in 0.1 M sodium phosphate buffer at pH 7. The spectra were obtained with Raman excitation at 229 nm. The band at 932 cm^{-1} corresponds to sodium perchlorate, which was used as an internal standard.

Journal of RAMAN SPECTROSCOPY

Table 1. Positions (in cm^{-1}) of the resonance Raman bands of NATA in water and Trp53 in wt barstar and in the W38FW44FC82A mutant variant of barstar

	NATA	WT	W38FW44FC82A
W28	N[a]	746	746
W18	761	762	760
New band	N[a]	780	778
W17	880	880	880
W16	1010	1010	1010
W10	1233	1226	1224
W8	1304	1307	1306
W7	1340	1340	1332
W7	1361	1365	1368
W4	1461	1462	1463
W5	1496	1496	1495
W3	1556	1557	1556

[a]N—not observed in NATA.

to 1226 cm^{-1} in wt barstar. Of the Fermi doublet (W7), the band at 1340 cm^{-1} broadens, and the second component of the doublet upshifts from 1361 cm^{-1} in water to 1365 in the protein. There is also a concurrent increase in the intensity ratio ($R = I_{\sim 1360}/I_{\sim 1340}$) of the doublet. An increase in the ratio of intensities of the Fermi doublet correlates with an increase in the hydrophobicity of the Trp local environment.[74,75] This suggests that at least one of the Trp residues in barstar must be in a hydrophobic environment. The spectrum of W38FW44FC82A shows similar characteristics in the W7, W10 and W18 regions of the spectrum. The fact that the mutant possesses only Trp53 confirms that the unusual spectral characteristics of barstar arise from this residue.

The correlation between environmental interactions and the Raman band positions and intensities of Trp has been systematically examined.[38,74,76–80] It is well known that the overall Raman cross section of Trp decreases with an increase in water accessibility to the side chain.[77] To get insight into the interactions of Trp53 with the local environment in barstar, we further characterized the UVRR spectrum of the single-Trp mutant protein, W38FW44FC82A. Table 2 includes the total differential Raman cross sections of the W3, W16 and W17 bands of Trp53 in this mutant protein and NATA. The overall cross sections of the Trp53 bands in barstar are greater than those of NATA. The intensity difference correlated well with the study of Chi *et al.*[77] in which the intensity of the bands of Trp in horse heart metmyoglobin decreases threefold during pH denaturation and the accompanying increase in the solvent accessibility of Trp. Fluorescence quenching experiments on barstar indicate that Trp53 is solvent inaccessible in the native state.[25] Thus, we ascribe the increase in the cross sections of Raman bands of Trp53 with respect to those of NATA in water to the solvent excluded environment in the core of native barstar where Trp53 is located.

Table 2. Total differential Raman cross sections of some bands of NATA in water and of Trp53 in the W38FW44FC82A mutant variant of barstar, obtained at 229-nm excitation wavelength

	Raman cross section ($Å^2$/molecule•str × 10^8)		
	W17	W16	W3
NATA	0.25	0.72	0.89
W38FW44FC82A	0.81	2.12	2.31

The W3 band of Trp53 appears at 1556 cm^{-1}. The wavenumber of the W3 band of Trp is correlated with the absolute value of the dihedral angle of the side chain, $\chi^{2,1} \equiv C_\alpha—C_\beta—C_3=C_2$[78–80] and is used as a marker of Trp conformation. This correlation between band position and side-chain dihedral angle $\chi^{2,1}$ implies an angle of 110° for Trp53 in barstar in solution. However, the value of the dihedral angle of Trp53 obtained from the crystal structure of barstar is about 46°. It is possible that the structure of Trp53 is different in solution and in the crystal. It is also likely that this discrepancy in the dihedral angle is because of altered normal mode composition of the W3 band, due to the highly constrained geometry of Trp53[25] in the protein and that the band does not, consequently, follow the general W3 position-dihedral angle correlation.

In the spectrum of W38FW44FC82A, an intense band appears at 778 cm^{-1}, and the band at 746 cm^{-1} that was a shoulder in the spectrum of wt barstar is better defined. The band at 762 cm^{-1} suffers a decrease in the relative intensity in comparison with other bands of the spectrum. Alterations in the W18 band region of Trp are observed in other proteins as well. Sanchez *et al.* observed that during refolding of the membrane protein OmpA, the spectrum of Trp15 has extra band at 778 cm^{-1} in the W18 region which increased in intensity with folding.[81] The origin of this new band was ascribed to a cation–π interaction between the side chain of Trp15 and lipid head groups of the membrane. The interpretation was supported by an extensive study by the same research group on model indole crown ethers which showed similar changes in the W18 region upon the addition of different cations.[82] The additional bands in the W18 region were assigned to hydrogen out-of-plane (HOOP) vibrations and in particular to vibrations of the hydrogen attached to the C2 carbon.[83] It was suggested that the distortion of the π-electron density of the indole ring due to interaction with a cation makes the HOOP vibrations Raman active. Surprisingly, the difference spectra in the absence and presence of cations show relative maxima at similar position than the new bands found in barstar. For example, the relative maxima for these bands in the case of Na^+ occur at 744 and 779 cm^{-1}. The position and intensity of the vibration at 746 cm^{-1} (W28 mode) in barstar are similar in origin and arise from HOOP vibrations of the benzene ring of indole.[83–85]

To get more information on the origin of these two new bands (778 cm^{-1} and 746 cm^{-1}), we carried out an isotope labeling experiment with H/D exchange by dissolving barstar in D_2O solution. The UVRR spectrum of the W38FW44FC82A mutant variant upon H/D exchange (Fig. 2) shows that the intensity and position of 778 cm^{-1} band do not undergo a significant change in D_2O, and that the band at 746 downshifts to 736 cm^{-1}. This implies that the later has contribution from N–H vibration. This downshift could be due to either hydrogen bonding of the hydrogen of the N–H group or due to distortion of the indole ring. The strength of the hydrogen bond of the NH group of the indole ring can be independently inferred from the position of the W17 band. The position of the W17 band downshifts with the increase in the strength of the N–H hydrogen bond with other residues.[74] The fact that in barstar the position of the W17 band is similar to that observed for NATA in water implies that there is no hydrogen bond formed by the N–H group. Thus, resonance enhancement of the HOOP mode at 746 cm^{-1} is due to distortion of the benzene ring of the indole and not due to altered hydrogen bond strength.

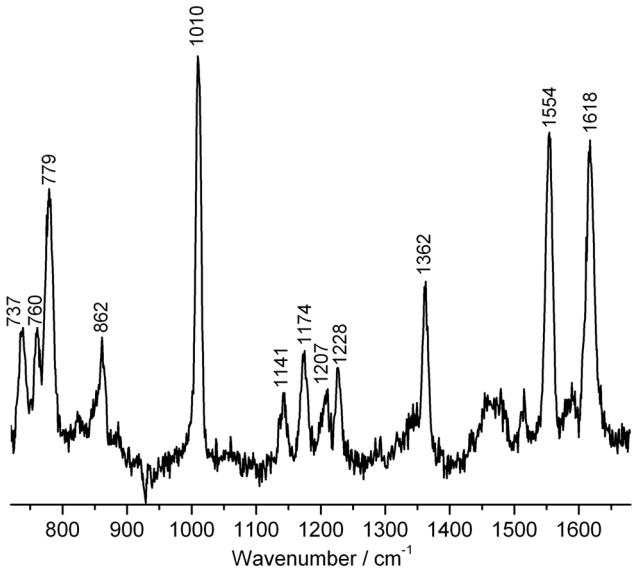

Figure 2. UVRR spectrum of the W38FW44FC82A mutant variant of barstar in 0.1 M sodium phosphate buffer prepared in D_2O obtained with Raman excitation with light of wavelength 229 nm.

The crystal structure of barstar (PDB 1A19[31]) shows that the nearest residue with a positive charge for a potential cation–π interaction with Trp53 is Arg54. However, the guanidinium group of Arg54 is about 10 Å away from the C2 carbon of the Trp53 indole ring. Hence, an energetically favorable cation-π interaction is unlikely.[87] However, there is an edge-to-face orientation between Phe56 and the indole ring of Trp53. One of the hydrogens of Phe56 is placed over the benzene ring and another over the pyrrole ring at distances of ~2.5 Å and 2.2 Å from the ring plane, respectively (Fig. 3(a)).These distances are shorter than the maximum distance suggested for the occurrence of a CH–π interaction: Nishio *et al.* set the distance at 3.05 Å, and Brandl *et al.* at 4.0 Å.[59,60,88] This edge-to-face CH–π interaction between two CH groups of Phe56 and the π-electron density of the side chain of Trp53 may cause effects in the W18 region of the UVRR spectrum similar to a cation–π interaction.[89] Although the changes found in the W18 region of Trp53 are qualitatively similar to those found for indole crown ethers and for Trp15 in the protein OmpA, there are clearly quantitative differences. The changes in the intensities of the new bands in the former are much more prominent than in the later. This may suggest more distortion of the π-electron density distribution in Trp53. For example, in the case of indole crown ethers, it was found that only the pyrrole ring is involved in the cation–π interaction.[83] In the case of Trp53 in barstar, both the benzene and pyrrole rings interact with the CH groups of Phe56.

The distances of the carbons of the CH groups of Phe56 to the benzene ring and pyrrole ring of Trp53 fall within the lower limits of those found in surveys of protein crystal structures for CH–π interactions. A survey of crystal structures by Brandl *et al.* showed that the number of CH–π interactions that occur between 3.0 Å and 3.5 Å is only a few percent of the total of the number of CH–π interactions.[60] In another study, a similar result was found for the occurrence of the CH–π interaction between methyl groups and the six-carbon rings of the aromatic residues Trp, Phe and Tyr. Though UVRR spectroscopy is extensively employed for studying protein structure and dynamics, the low wavenumber occurrence of the CH–π interaction within this range of distances could explain why such spectral characteristics have not been reported previously in the spectra of proteins.

The relative intensity ratios of the Fermi doublet of Trp53 are altered in barstar. Compared to R = 1.33 in NATA, the ratio for Trp53 in barstar is 1.9 which corresponds to a hydrophobic environment around Trp53. This is in agreement with the observed crystal structure of barstar in which Trp53 is surrounded by several aliphatic amino acid residues (Leu16, Leu51, Leu71, Ile5 and Val70). The positions and widths of these two bands also indicate an unusual interaction of the Trp53 side chain with its local environment. The first component of the doublet broadens, while the second component upshifts from 1361 to 1368 cm^{-1}.

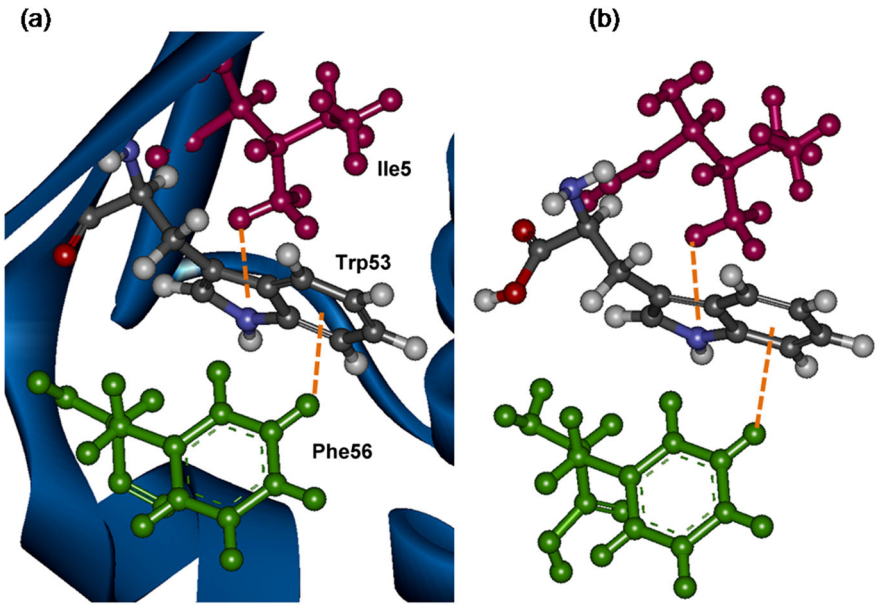

Figure 3. Distance between CH group of Phe56 and Ile5 and indole ring and pyrrole ring center of Trp53, respectively, in (a) mutant barstar (PDB 1A19) and (b) wB97xD optimized structure.

Similar effects have been noted recently by Sanchez *et al.* in the position and width of the W7 bands of Trp15 in the protein OmpA.[81] On folding, the first component of W7 downshifts (7 cm^{-1}), while the second component upshifts (3 cm^{-1}) with respect to the unfolded state. The bands also became broader in the folded protein than they are in the unfolded protein. This similarity in the Fermi doublets, as well as that of W18 mentioned earlier, between Trp53 in barstar and Trp15 in OmpA stresses the possibility that the indole ring of Trp53 in barstar is involved in a CH–π interaction with Phe56. Wen *et al.* found that the spectrum of native filamentous virus Pf3 also shows an elevated value of the second component of the Fermi doublet at a wavenumber of 1370 cm^{-1} which they ascribed to the presence of a cation–π interaction between the indole ring of Trp38 and residues Arg37 or Lys40 in that protein.[89]

In a recent study of the synthetic peptide TrpZip2 and some of its variants, Schlamadinger *et al.* demonstrated that the Fermi doublet region is sensitive to edge-to-face interaction between a pair of Trp.[90] It was suggested that the interaction between one hydrogen of the benzene ring of Trp11 with the pyrrole ring of Trp2 (acting as acceptor) likely produces perturbation in some HOOP vibrations that contribute to the combination bands of Trp11. It was mentioned that perturbations in the Fermi doublet region of Trp2 may also occur because its pyrrole ring is directly involved in the interaction. Though this study demonstrated the sensitivity of the UVRR spectroscopy to monitor these kinds of interactions, it is difficult to determine the specific contribution of Trp2 and Trp11 to the spectrum. In our study, the spectral characteristics come only from Trp53 where its side chain act as a donor in the edge-to-face interaction with Phe56.

In another study, the spectrum of Trp182 in bacteriorhodopsin at 244-nm excitation wavelength showed a triplet in the W7 region with an additional band at 1370 cm^{-1}.[91] Taking into account previous FTIR studies of bacteriorhodopsin,[92] it was suggested that strong steric repulsion between the Trp182 side chain and the methyl groups of retinal might upshift the W28 mode, and then the combination with the W29 vibration at about 620 cm^{-1} would produce the new band in the W7 region. However, the position of W28 band in barstar (746 cm^{-1}) is close to the position reported for Trp and acetyl tryptophan ethyl ester in different solvents (742 cm^{-1}).[92] Thus, the upshift that we observe in the second component of the Fermi doublet is unlikely to arise from steric repulsion.

Another unusual characteristic in the spectrum of the barstar is the position of the W10 band at 1224 cm^{-1}downshifted by 9 cm^{-1} with respect to NATA in water. The W10 band is expected to be hydrogen bond sensitive due to the normal mode contribution from N-H bending.[75] Taking into account that W17, a hydrogen bond marker discussed earlier does not shift in position with respect to that of NATA, the downshift of the W10 band must be due to some other interaction of Trp53 with the surrounding amino acid residues. Downshifts in the W10 band have been observed only in a few proteins. Besides showing the shift in the W7 band, the spectrum of native filamentous virus Pf3 reported by Wen *et al.* showed a downshift in the W10 band of Trp38 up to 1228 cm^{-1}.[89] This shift is assigned to interaction of the Trp side chain with a cationic group. In barstar, the indole ring of Trp53 is sandwiched between the side chains of Phe56 and Ile5. The carbon of one of the methyl groups of Ile5 is at a distance of about 3.4 Å from the nitrogen of the pyrrole ring of Trp53, and they could have a steric interaction producing the shifts on the W10 band in the spectrum of barstar. Thus, the perturbed W10 band reflects both CH–π as well as steric interactions. These data show that Trp53 in the core of barstar is tightly packed through CH–π interactions that constrain the rotation of Trp53.

In a study of barstar by using MD simulation, it was found that the side chain of Phe74 has freedom to move but the ring of Phe56 does no flip.[30] This result agrees with a more recent study by using ^{19}F NMR spectroscopy where it was determined that the rotation of the side chain of Phe56 is restricted.[29] It was suggested that the restriction may occur due a favorable interaction between the positive partial charges of the hydrogen atoms of Phe56 with the electronic density of the Trp53 side chain. Computational calculations of the interaction energies of benzene-indole dimers demonstrate that when the indole ring acts as hydrogen acceptor, the most stable configuration is that in which two hydrogens of benzene are placed over the center of the six and five member rings of indole forming a T-shape configuration.[93,94] These results also suggest a favored interaction between the positive partial charge of hydrogens of Phe56 side chain and the π electronic density of indole ring of Trp53 in barstar. The normal mode calculation carried out previously using indole crown ether as model demonstrated that the interaction of a positive charge with the indole ring produces alterations in the HOOP and W18 vibrational modes.[82] This result was also corroborated by NMR experiments. These studies and the similarity of spectral characteristics of the UVRR spectra of other systems that show interactions between positive charge with the electronic density of indole ring strongly support the interpretation of our results.

Here, we carried out quantum chemical calculations to understand the origin of the characteristics of the experimental UVRR spectrum of Trp53 in barstar. For determining the equilibrium distance and configuration of the Trp53–Phe56 complex, the PES was scanned along relevant coordinates as described in the Methods section. Figure S4a (Supporting Information) shows that the $R_{CH-\pi}$, distance corresponding to the minimum energy, is 2.74 Å. For these calculations, the value of the dihedral angle between Phe56 and Trp53, $\phi_{Phe-Trp,}$, was taken from the crystal structure and kept fixed (160.5°) during the scan. Variations of the $R_{CH-\pi}$ distance from 2.64 Å to 2.94 Å do not produce major changes on the energy of the complex, and the relative energy remains approximately constant (within 0.5 kcal/mol). The energy dependence of the complex with respect to the dihedral angle, $\phi_{Phe-Trp}$, was also determined by varying the angle. The relative energies of different structural conformations of the Trp53–Phe56 complex do not change more than 0.5 kcal/mol along the $\phi_{Phe-Trp}$ coordinate. This insensitivity of the CH–π interaction energy to the ring rotation coordinate implies that it is a well-defined local minimum on the PES of the Trp53–Phe56 complex. The value of the $\phi_{Phe-Trp}$ for which the PES has a minimum is in agreement with the value obtained from the reported crystal structure of barstar. During the calculations of the rigid PES scan along $\phi_{Phe-Trp}$, the distance $R_{CH-\pi}$ varies from 2.71 to 2.64 Å.

There are typically three parameters used to define a CH–π interaction in a non-covalent complex[95]: (1) the distance between the C–H hydrogen and center of π system ($R_{CH-\pi}$) is in the range of 2.6–3.0 Å, (2) the distance between the carbon atom of C–H donor and the center of π system ($R_{C-\pi}$) is ≤4.5 Å and (3) the angle between the C–H bond and center of π system ($\phi_{C-H-\pi}$) is ≥120°. The values of these parameters on the optimized structure of the Trp53–Phe56 complex are $R_{CH-\pi}$ = 2.74 Å, $R_{C-\pi}$ = 3.6 Å and ϕ_{C-}

$_{H-\pi}$ = 130°. These values fall within the range established for the complex to form a favorable CH–π interaction.

Similar calculations were carried out by including Ile5 to the Trp53–Phe56 complex. Potential energy change along the R_{CH-Py} distance was computed by keeping $R_{CH-\pi}$ and $\phi_{Phe-Trp}$ fixed at 2.74 Å and −160.5°, respectively. The value of R_{CH-Py} for which the potential well has a minimum is 2.9 Å (Fig. S4b (Supporting Information)) and this distance is close to the value obtained from the crystal structure (2.85 Å). The result suggests that the structure of the Trp53–Phe56–Ile5 complex indeed is on a local minimum. Energy minimization of the structure of the complex was then carried out with the initial structure taken from the rigid PES scan discussed above. During the partial geometry optimization, Ile5 and Phe56 residues, and the backbone of Trp53 were kept fixed while the indole ring of Trp53 was allowed to relax. Vibrational wavenumber calculation using the obtained optimized structure does not yield imaginary wavenumbers, implying that the geometry is indeed a true minimum. The geometric parameters of benzene and pyrrole rings in free Trp and of Trp53 in the Trp53–Phe56–Ile5 complex are tabulated in Table S1 (Supporting Information).

The vibrational wavenumbers and the absolute Raman and IR activities for each normal mode of Trp are shown in Table S2 (Supporting Information). Calculations predict mixing of HOOP vibrations with many of the ring breathing modes of Trp53. The computed Raman activity for the W18 mode in Trp53 is fourfold smaller than that of free Trp. The computed Raman activity for this mode in Trp53 is fourfold smaller than that of free Trp. The experimental relative intensity (I_{W18}/I_{W16}) for Trp53 in the mutant W38FW44FC82A of barstar also shows a drastic decrease with respect to NATA in water. Computed normal modes show that the strong W18 mode of Trp, a pure in-plane ring breathing vibration in the case of free Trp, couples to out-of-plane motions of ring carbons for Trp53 in barstar. The computed Raman activities for the modes of Trp53 show increase and decrease of the intensity of the 746 cm^{-1} and 762 cm^{-1} bands, respectively, in comparison with the values obtained for free Trp.

The presence of CH–π interactions in proteins has been studied by statistical analysis of the crystal structures of several proteins, and it has been also determined that these interactions play an important role in the function and stability of proteins.[54–63] The experimental challenge is the direct detection of CH–π interactions in proteins. Past attempts have resorted to the use of synthesized molecules to characterize these interactions. Recently, a direct observation of a CH–π (methyl-π) interaction in proteins was made with NMR spectroscopy using aromatic amino acid residues as π-acceptors.[88] Though the CH–π interactions are similar in nature to the vdW interactions, they also have some differences. While the former are specific and have certain directionality, the later are non-specific and do not depend on the orientation of the interacting groups. Example of the dependence on the orientation of the CH–π interaction is the edge-to-face configuration between aromatic amino acids found in proteins. Burley *et al.* in a survey of available crystal structures of 34 proteins found that there is a preference for the side chain of aromatic amino acids to be in a perpendicular configuration.[96]

Here we have reported for the first time, using Raman spectroscopy, a CH–π interaction involving a Trp residue buried in the protein core. The results demonstrate the sensitivity of UVRR spectroscopy for the detection of CH–π interactions in proteins, and they open up future possibilities for studies of the role of the dispersion forces in the folding and unfolding reactions of proteins.

Conclusions

In summary, the vibrational spectrum of Trp53 in barstar provides clear evidence for packing interactions that lead to structural distortion and motional restraint by neighboring residues of the Trp. We have determined that the unique spectrum of Trp53 is due to the interaction of the π-electron density of the indole ring of Trp53 with the CH groups of Phe56 and to the steric interaction of one methyl group of Ile5. Ile5 is a part of β-strand 1 of barstar while Trp53 and Phe56 are part of β-strand 2 and α-helix 3, respectively. Considering that Trp53 and Phe56 are residues located close to each other in the primary sequence, it is likely that the CH–π interaction between them forms early in the folding process. Such CH–π interactions are difficult to observe experimentally, and this is a rare instance when a critical packing interaction has been identified within a protein widely studied for its native structure, folding and unfolding properties.

The fact that the residues Ile5, Trp53 and Phe56 belong to different secondary structural units in the protein will allow monitoring of the formation of tertiary structures during the folding reaction of barstar.[96] We are currently examining the relative hierarchy of secondary structure formation *versus* core packing during folding and unfolding in barstar using these unique vibrational signatures of Trp53.

Acknowledgements

We thank Santosh Kumar Jha for providing us with the proteins used in this study. JBU is a recipient of a JC Bose Fellowship from the Government of India. MJP is a recipient of the Innovative Young Biotechnologist Award from the Government of India. This work was funded by the Tata Institute of Fundamental Research, the Department of Biotechnology (MJP) and the Department of Science and Technology, Government of India (JBU).

References

[1] K. A. Dill, *Biochemistry* **1990**, *29*, 7133.
[2] F. M. Richards, W. A. Lim, *Q. Rev. Biophys.* **1993**, *26*, 423.
[3] J. M. Chen, W. E. Stites, *Biochemistry* **2001**, *40*, 15280.
[4] G. S. Ratnaparkhi, R. Varadarajan, *Biochemistry* **2000**, *39*, 12365.
[5] J. M. Chen, W. E. Stites, *Biochemistry* **2001**, *40*, 14004.
[6] F. M. Richards, *Annu. Rev. Biophys. Bioeng.* **1977**, *6*, 151.
[7] C. Chothia, *Annu. Rev. Biochem.* **1984**, *53*, 537.
[8] G. D. Rose, R. Wolfenden, *Annu. Rev. Biophys. Biomol. Struct.* **1993**, *22*, 381.
[9] B. W. Matthews, *Adv. Protein Chem.* **1995**, *46*, 249.
[10] W. A. Lim, R. T. Sauer, *J. Mol. Biol.* **1991**, *219*, 359.
[11] W. A. Lim, R. T. Sauer, *Nature* **1989**, *339*, 31.
[12] M. Karpusas, W. A. Baase, M. Matsumura, B. W. Matthews, *Proc. Natl. Acad. Sci. U. S. A.* **1989**, *86*, 8237.
[13] J. B. Holder, A. F. Bennett, J. M. Chen, D. S. Spencer, M. P. Byrne, W. E. Stites, *Biochemistry* **2001**, *40*, 13998.
[14] R. L. Baldwin, C. Frieden, G. D. Rose, *Proteins* **2010**, *78*, 2725.
[15] S. K. Jha, J. B. Udgaonkar, *Proc. Natl. Acad. Sci. U. S. A.* **2009**, *106*, 12289.
[16] A. Reiner, P. Henklein, T. Kiefhaber, *Proc. Natl. Acad. Sci. U. S. A.* **2010**, *107*, 4955.
[17] T. Kiefhaber, A. M. Labhardt, R. L. Baldwin, *Nature* **1995**, *375*, 513.
[18] S. D. Hoeltzli, C. Frieden, *Proc. Natl. Acad. Sci. U. S. A.* **1995**, *92*, 9318.
[19] K. Sridevi, J. B. Udgaonkar, *Biochemistry* **2003**, *42*, 1551.
[20] V. R. Agashe, M. C. R. Shastry, J. B. Udgaonkar, *Nature* **1995**, *377*, 754.
[21] K. Sridevi, J. B. Udgaonkar, *Biochemistry* **2002**, *41*, 1568.

[22] K. Sridevi, J. Juneja, A. K. Bhuyan, G. Krishnamoorthy, J. B. Udgaonkar, *J. Mol. Biol.* **2000**, *302*, 479.
[23] B. R. Rami, J. B. Udgaonkar, *Biochemistry* **2002**, *41*, 1710.
[24] B. R. Rami, G. Krishnamoorthy, J. B. Udgaonkar, *Biochemistry* **2003**, *42*, 7986.
[25] R. Swaminathan, U. Nath, J. B. Udgaonkar, N. Periasamy, G. Krishnamoorthy, *Biochemistry* **1996**, *35*, 9150.
[26] K. K. Sinha, J. B. Udgaonkar, *J. Mol. Biol.* **2005**, *353*, 704.
[27] U. Nath, J. B. Udgaonkar, *Biochemistry* **1997**, *36*, 8602.
[28] M. C. R. Shastry, J. B. Udgaonkar, *J. Mol. Biol.* **1995**, *247*, 1013.
[29] H. Li, C. Frieden, *Biochemistry* **2007**, *46*, 4337.
[30] K. B. Wong, V. Daggett, *Biochemistry* **1998**, *37*, 11182.
[31] G. S. Ratnaparkhi, S. Ramachandran, J. B. Udgaonkar, R. Varadarajan, *Biochemistry* **1998**, *37*, 6958.
[32] P. L. Wintrode, Y. V. Griko, P. L. Privalov, *Protein Sci.* **1995**, *4*, 1528.
[33] M. J. Lubienski, M. Bycroft, S. M. V. Freund, A. R. Fersht, *Biochemistry* **1994**, *33*, 8866.
[34] K. B. Wong, S. M. V. Freund, A. R. Fersht, *J. Mol. Biol.* **1996**, *259*, 805.
[35] M. Ludwig, S. A. Asher, *J. Am. Chem. Soc.* **1988**, *110*, 1005.
[36] S. P. A. Fodor, R. A. Copeland, C. A. Grygon, T. G. Spiro, *J. Am. Chem. Soc.* **1989**, *111*, 5509.
[37] J. A. Sweeney, S. A. Asher, *J. Phys. Chem.* **1990**, *94*, 4784.
[38] T. Jordan, J. C. Austin, T. G. Spiro, Ultraviolet resonance Raman studies of proteins and related model compounds, John Wiley and Sons Ltd.: New York, **1993**.
[39] I. K. Lednev, A. S. Karnoup, M. C. Sparrow, S. A. Asher, *J. Am. Chem. Soc.* **1999**, *121*, 8074.
[40] Z. H. Chi, S. A. Asher, *Biochemistry* **1998**, *37*, 2865.
[41] Z. H. Chi, S. A. Asher, *Biochemistry* **1999**, *38*, 8196.
[42] Z. H. Chi, X. G. Chen, J. S. W. Holtz, S. A. Asher, *Biochemistry* **1998**, *37*, 2854.
[43] S. Takahashi, S. R. Yeh, T. K. Das, C. K. Chan, D. S. Gottfried, D. L. Rousseau, *Nat. Struct. Biol.* **1997**, *4*, 44.
[44] S. R. Yeh, D. L. Rousseau, *J. Biol. Chem.* **1999**, *274*, 17853.
[45] N. Haruta, T. Kitagawa, *Biochemistry* **2002**, *41*, 6595.
[46] C. Y. Huang, G. Balakrishnan, T. G. Spiro, *Biochemistry* **2005**, *44*, 15734.
[47] G. Balakrishnan, Y. Hu, M. A. Case, T. G. Spiro, *J. Phys. Chem. B* **2006**, *110*, 19877.
[48] C. Y. Huang, G. Balakrishnan, T. G. Spiro, *J. Raman Spectrosc.* **2006**, *37*, 277.
[49] A. V. Mikhonin, S. V. Bykov, N. S. Myshakina, S. A. Asher, *J. Phys. Chem. B* **2006**, *110*, 1928.
[50] S. Hashimoto, J. Fukasaka, H. Takeuchi, *J. Raman Spectrosc.* **2001**, *32*, 557.
[51] G. Balakrishnan, Y. Hu, G. M. Bender, Z. Getahun, W. F. DeGrado, T. G. Spiro, *J. Am. Chem. Soc.* **2007**, *129*, 12801.
[52] G. Balakrishnan, C. L. Weeks, M. Ibrahim, A. V. Soldatova, T. G. Spiro, *Curr. Opin. Struct. Biol.* **2008**, *18*, 623.
[53] Z. Ahmed, I. A. Beta, A. V. Mikhonin, S. A. Asher, *J. Am. Chem. Soc.* **2005**, *127*, 10943.
[54] O. Takahashi, Y. Kohno, M. Nishio, *Chem. Rev.* **2010**, *110*, 6049.
[55] M. Harigai, M. Kataoka, Y. Imamoto, *J. Am. Chem. Soc.* **2006**, *128*, 10646.
[56] M. Harigai, M. Kataoka, Y. Imamoto, *Photochem. Photobiol.* **2008**, *84*, 1031.
[57] T. Ozawa, K. Okazaki, K. Kitaura, *J. Comput. Chem.* **2011**, *32*, 2774.
[58] R. Bhattacharyya, P. Chakrabarti, *J. Mol. Biol.* **2003**, *331*, 925.
[59] Y. Nakagawa, K. Irie, R. C. Yanagita, H. Ohigashi, K. Tsuda, *J. Am. Chem. Soc.* **2005**, *127*, 5746.
[60] M. Brandl, M. S. Weiss, A. Jabs, J. Suhnel, R. Hilgenfeld, *J. Mol. Biol.* **2001**, *307*, 357.
[61] P. Chakrabarti, U. Samanta, *J. Mol. Biol.* **1995**, *251*, 9.
[62] Y. Umezawa, M. Nishio, *Bioorg. Med. Chem.* **1998**, *6*, 493.
[63] M. Nishio, M. Hirota, Y. Umezawa, The CH/π interaction. Evidence, Nature, and Consequences, Wiley-VCH, New York, **1998**.
[64] S. Tsuzuki, A. Fujii, *Phys. Chem. Chem. Phys.* **2008**, *10*, 2584.
[65] K. Shibasaki, A. Fujii, N. Mikami, S. Tsuzuki, *J. Phys. Chem. A* **2007**, *111*, 753.
[66] A. Fujii, K. Shibasaki, T. Kazama, R. Itaya, N. Mikami, S. Tsuzuki, *Phys. Chem. Chem. Phys.* **2008**, *10*, 2836.
[67] R. Khurana, J. B. Udgaonkar, *Biochemistry* **1994**, *33*, 106.
[68] K. K. Sinha, J. B. Udgaonkar, *J. Mol. Biol.* **2007**, *370*, 385.
[69] A. B. Myers, Excited electronic state properties from ground-state resonance Raman intensities, Wiley, New York, **1995**.
[70] J. M. Dudik, C. R. Johnson, S. A. Asher, *J. Chem. Phys.* **1985**, *82*, 1732.
[71] J. D. Chai, M. Head-Gordon, *Phys. Chem. Chem. Phys.* **2008**, *10*, 6615.
[72] L. Goerigk, S. Grimme, *Phys. Chem. Chem. Phys.* **2011**, *13*, 6670.
[73] K. E. Riley, M. Pitonak, P. Jurecka, P. Hobza, *Chem. Rev.* **2010**, *110*, 5023.
[74] T. Miura, H. Takeuchi, I. Harada, *Biochemistry* **1988**, *27*, 88.
[75] D. E. Schlamadinger, J. E. Gable, J. E. Kim, *J. Phys. Chem. B* **2009**, *113*, 14769.
[76] H. Takeuchi, *Biopolymers* **2003**, *72*, 305.
[77] Z. H. Chi, S. A. Asher, *J. Phys. Chem. B* **1998**, *102*, 9595.
[78] T. Miura, H. Takeuchi, I. Harada, *J. Raman Spectrosc.* **1989**, *20*, 667.
[79] T. Maruyama, H. Takeuchi, *J. Raman Spectrosc.* **1995**, *26*, 319.
[80] L. J. Juszczak, R. Z. B. Desamero, *Biochemistry* **2009**, *48*, 2777.
[81] K. M. Sanchez, G. P. Kang, B. J. Wu, J. E. Kim, *Biophys. J. 100*, 2121.
[82] D. E. Schlamadinger, M. M. Daschbach, G. W. Gokel, J. E. Kim, *J. Raman Spectrosc.* **2010**, *42*, 633.
[83] S. W. Bunte, G. M. Jensen, K. L. McNesby, D. B. Goodin, C. F. Chabalowski, R. M. Nieminen, S. Suhai, K. J. Jalkanen, *Chem. Phys.* **2001**, *265*, 13.
[84] H. Takeuchi, I. Harada, *Spectrochim. Acta Mol. Biomol. Spectrosc.* **1986**, *42*, 1069.
[85] A. Combs, K. McCann, D. Autrey, J. Laane, S. A. Overman, G. J. Thomas, *J. Mol. Struct.* **2005**, *735*, 271.
[86] J. P. Gallivan, D. A. Dougherty, *Proc. Natl. Acad. Sci. U. S. A.* **1999**, *96*, 9459.
[87] M. Nishio, Y. Umezawa, M. Hirota, Y. Takeuchi, *Tetrahedron* **1995**, *51*, 8665.
[88] M. J. Plevin, D. L. Bryce, J. Boisbouvier, *Nat. Chem.* **2010**, *2*, 466.
[89] Z. Q. Wen, G. J. Thomas, *Biochemistry* **2000**, *39*, 3184.
[90] D. E. Schlamadinger, B. S. Leigh, J. E. Kim. *J. Raman Spectrosc* **2012**, *43*, 1459.
[91] S. Hashimoto, K. Obata, H. Takeuchi, R. Needleman, J. K. Lanyi, *Biochemistry* **1997**, *36*, 11583.
[92] P. Roepe, D. Gray, J. Lugtenburg, E. M. M. Vandenberg, J. Herzfeld, K. J. Rothschild, *J. Am. Chem. Soc.* **1988**, *110*, 7223.
[93] Y. Geng, T. Takatani, E. G. Hohenstein, C. D. Sherrill, *J. Phys. Chem. A* **2010**, *114*, 3576.
[94] S. Karthikeyan, S. Nagase, *J. Phys. Chem. A* **2012**, *116*, 1694.
[95] N. Mohan, K. P. Vijayalakshmi, N. Koga, C. H. Suresh, *J. Comput. Chem.* **2010**, *31*, 2874.
[96] S. K. Burley, G. A. Petsko, *Science* **1985**, *229*, 23.
[97] Gaussian 09, Revision D.01, M. J. Frisch, G. W. Trucks, H. B. Schlegel, G. E. Scuseria, M. A. Robb, J. R. Cheeseman, G. Scalmani, V. Barone, B. Mennucci, G. A. Petersson, H. Nakatsuji, M. Caricato, X. Li, H. P. Hratchian, A. F. Izmaylov, J. Bloino, G. Zheng, J. L. Sonnenberg, M. Hada, M. Ehara, K. Toyota, R. Fukuda, J. Hasegawa, M. Ishida, T. Nakajima, Y. Honda, O. Kitao, H. Nakai, T. Vreven, J. A. Montgomery Jr., J. E. Peralta, F. Ogliaro, M. Bearpark, J. J. Heyd, E. Brothers, K. N. Kudin, V. N. Staroverov, R. Kobayashi, J. Normand, K. Raghavachari, A. Rendell, J. C. Burant,S. S. Iyengar,J. Tomasi, M. Cossi, N. Rega, J. M. Millam, M. Klene, J. E. Knox, J. B. Cross, V. Bakken, C. Adamo, J. Jaramillo, R. Gomperts, R. E. Stratmann, O. Yazyev, A. J. Austin, R. Cammi, C. Pomelli, J. W. Ochterski, R. L. Martin, K. Morokuma, V. G. Zakrzewski, G. A. Voth, P. Salvador, J. J. Dannenberg, S. Dapprich, A. D. Daniels, Ö. Farkas, J. B. Foresman, J. V. Ortiz, J. Cioslowski, D. J. Fox. Gaussian, Inc: Wallingford CT. **2009**.

Supporting information

Additional supporting information may be found in the online version of this article at the publisher's web site.